V European Conference on Computational Fluid Dynamics
ECCOMAS CFD 2010
J. C. F. Pereira and A. Sequeira (Eds)
Lisbon, Portugal,14-17 June 2010

EFFECTS OF MODELING UNCERTAINTIES IN CONDENSING WET-STEAM FLOWS THROUGH SUPERSONIC NOZZLES

Michele Giordano*, Samuel J. Hercus† and Paola Cinnella†

*Dipartimento di Ingegneria dell'Innovazione,
Università del Salento
via per Monteroni, 73100, Lecce, Italy
e-mail: michele.giordano@unisalento.it
†Laboratoire DynFluid
Arts et Métiers–ParisTech 151 bd. de l'Hôpital, 75013, Paris, France
e-mail: {samuel.hercus,paola.cinnella}@paris.ensam.fr

Key words: Wet-steam, uncertainty quantification, polynomial chaos, moment method

Abstract. *A systematic analysis of the effect of modeling uncertainties in the simulation of wet steam flows is performed through the coupling of a wet steam flow solver with an uncertainty quantification method. A Probabilistic Collocation Method (PCM) is selected due to its non-intrusive nature and exponential convergence. Uncertainties affecting calibration coefficients in the droplet nucleation and growth models are propagated through the wet steam flow solver using the PCM approach The separated and coupled effect of such uncertainties is studied for condensing flows through both high-pressure and low-pressure quasi-1D supersonic nozzles.*

1 INTRODUCTION

Wet steam flows are typically modeled as multiphase gas droplet mixtures in which both vapor and liquid droplets coexist. In these flows, spontaneous nucleation leads to the formation of liquid droplets from vapor. A key point in the computation of this type of multiphase flow is the determination of the shape of the droplet spectrum. In a previous work, two of the present authors developed an inviscid numerical solver for wet steam flows based on the moment method.[1] The droplet size distribution is partly modeled through the resolution of transport equations for the lowest order moments of the droplet spectrum. This allows evaluation of the wetness fraction and the mean radius of the droplets. Past validations for wet steam flows through convergent-divergent nozzles show that the results are in good agreement with the available experimental data for pressure distributions. However, differences of up to 40% are observed for droplet properties such as the mean droplet diameter, which are directly influenced by nucleation and growth model parameters. These models require the specification of several thermo-physical properties of the liquid phase, along with calibration constants. For some of these parameters, the values encountered in the literature may vary significantly within very large intervals. For instance, in the case of the the condensation coefficient q_c for water, values between 10^{-3} and 1 have been reported. The condensation coefficient appears in the pre-exponential factor in the nucleation rate equation. Early experiments by Alty and MacKay[2] indicated values around 0.02-0.03, but it is now thought that these measurements were subject to large systematic errors and the general consensus is that q_c takes values close to 1.[3,4] Although the values of q_c are typically assumed as $q_c \approx 1$, all experimental evidence has been obtained with drop surfaces which are large on a molecular scale. For very small clusters, the value of q_c is almost certainly much less than 1.[5] Similarly, in the droplet growth rate model, an empirical parameter β appears which can take values between 0 and 5. This parameter was introduced by Young[6] to provide more flexibility in the model calibration phase for low-pressure nozzles. The classical value $\beta = 0$ is preferred for Wilson point pressures above 0.5 bar. Conversely, according to Young, comparisons with experimental data indicate better agreement between computed and experimental data for $\beta = 5$ if the Wilson point pressure is around 0.1 bar. The Wilson point is defined as the point of maximal subcooling along a streamline as well as the point where dry and condensing static pressure curves first separate. When experimental data are not available for calibration and for intermediate Wilson-point pressures, the adjustable parameter β is a strong contributor of uncertainty. In this case, uncertainty quantification is critical in evaluating the accuracy and precision of the CFD simulations.

The objective of the present work is to carry out a systematic analysis of the impact of model parameter uncertainties on the numerical solution of wet-steam solvers. The statistical output information is subsequently compared with experimental data. In recent years, research efforts have led to the development of several uncertainty quantification methods, which may be classified as non-intrusive or statistical (e.g., the Monte Carlo

method and the surface response method) or intrusive/non-statistical (e.g. polynomial chaos (PC) methods). Among these methodologies, considerable interest has been received by Generalized Polynomial Chaos (GPC) methods because of their high accuracy and computational efficiency compared to other methods. However, a principal disadvantage of the GPC is the intrusive nature of the approach, where the CFD code requires direct modification. Nevertheless, it is possible to develop non-intrusive formulations based on PC theory, such as probabilistic collocation and chaos collocation methods.[7–9] These non-intrusive methods may be coupled with a deterministic flow solver which can be considered as an external *black box*, and no modification of the CFD code is required. As a consequence, non-intrusive methods are more versatile than the intrusive approaches, since they may be applied to different problems just by changing the deterministic flow solver.

In this work, the Probabilistic Collocation Method (PCM) by Loeven et al.[7,8] is selected due to its non-intrusive nature and exponential convergence. Uncertainties affecting calibration coefficients in the droplet nucleation and growth models are propagated through the wet steam flow solver using the PCM approach. The separated and coupled effect of such uncertainties is studied for condensing flows through both high-pressure and low-pressure quasi-1D supersonic nozzles.

2 GOVERNING EQUATIONS

2.1 The Moment Method

In the present work, wet steam is modeled by means of the moment method. This approach[10–13] is based on the assumption that the full droplet spectrum in not required in most cases. In such cases, the correct coupling between vapor and liquid droplets is achieved by computing only the first few moments of the size distribution.

2.1.1 Mixture Conservation Equations

We solve the conservation equations for a two-phase mixture of vapor and fine droplets. These equations take the same form of their single phase counterparts. For inviscid, adiabatic wet-steam flows with zero inter-phase slip, the mass continuity, momentum and energy equations for the two-phase mixture in conservation variables are:

$$\frac{\partial \rho_m}{\partial t} + \nabla \cdot (\rho_m \mathbf{u}) = 0 \quad , \tag{1}$$

$$\frac{\partial}{\partial t}(\rho_m \mathbf{u}) + \nabla \cdot (\rho_m \mathbf{u}\,\mathbf{u}) + \nabla p = 0 \quad , \tag{2}$$

$$\frac{\partial}{\partial t}(\rho_m E) + \nabla \cdot (\rho_m E\,\mathbf{u}) + \nabla \cdot (p\mathbf{u}) = 0 \quad , \tag{3}$$

where $\mathbf{u}$ represents the common velocity field, ρ_m is the mixture density and E is the mixture total energy per unit mass. Their definitions are:

$$\frac{1}{\rho_m} = \frac{1-y}{\rho_v} + \frac{y}{\rho_l} \simeq \frac{1-y}{\rho_v} \quad , \tag{4}$$

$$E = e + \frac{1}{2}u^2 \quad , \quad \text{with} \quad e = (1-y)\, e_v + y\, e_l \quad , \tag{5}$$

with y the wetness fraction, i.e. the mass of liquid per unit mass of the mixture, and e equal to the internal energy per unit mass of the mixture. The subscripts m, v and l refer to mixture, vapor and liquid, respectively. The relation between mixture total energy E and total enthalphy H (both per unit mass) is given by:

$$H = E + \frac{p}{\rho_m} \quad , \tag{6}$$

since

$$\begin{aligned} H \quad &= (1-y)\, H_v + y\, H_l = (1-y)\, (E_v + p/\rho_v) + y\, (E_l + p/\rho_l) = \\ &= (1-y)\, E_v + y\, E_l + p\, ((1-y)/\rho_v + y/\rho_l) = E + p/\rho_m \quad . \end{aligned} \tag{7}$$

2.1.2 Moment Equations

A relevant benefit coming from the use of the moments of the droplet size distribution is that vapor-liquid heat and mass transfer can be accurately modeled by solving a few moment equations, rather than a larger number related to numerous droplet groups. The j^{th} moment of the droplet size distribution is defined as:

$$\mu_j = \int_0^\infty r^j f \, \mathrm{d}r \quad , \tag{8}$$

where f is the droplet number density function and r the droplet radius. Low order moments have a physical significance. In particular, μ_0 is equal to the total number of droplets per unit mass of mixture and μ_3 is proportional to the wetness fraction:

$$\mu_0 = n_T \quad , \quad \mu_3 = \frac{3}{4\pi\rho_l} y \quad . \tag{9}$$

For the droplet diameter, the Sauter mean diameter $d_{32} = \frac{2\,\mu_3}{\mu_2}$ is used. In order to determine y, an equation describing the evolution of μ_j is needed. The generic conservation equation for the j^{th} moment is given by:

$$\frac{\partial}{\partial t}(\rho_m \mu_j) + \nabla \cdot (\rho_m \mu_j \mathbf{u}) = j \rho_m \int_0^\infty r^{j-1} G f \, \mathrm{d}r + \rho_m J_* r_*^j \quad . \tag{10}$$

where G is the droplet growth rate. The definitions of the critical radius r_* and of the critical nucleation rate J_* come from the assumption that droplets form only at a critical radius r_*, so that the nucleation rate J can be written as Dirac-delta function:

$$J = J_* \delta(r - r_*) \quad . \tag{11}$$

Following the definition from Kelvin-Helmholtz, the critical radius r_* is given by:

$$r_* = \frac{2\sigma}{\rho_l \, RT_v \ln S} \approx \frac{2\sigma \, T_s(p)}{\rho_l \, h_{vl} \Delta T} \quad , \tag{12}$$

with σ the surface tension, $T_s(p)$ the saturation temperature at pressure p, $h_{vl} = h_v - h_l$ the specific enthalpy of evaporation and $\Delta T = T_s(p) - T_v$ the vapour subcooling. $S = \frac{p}{p_s(T_v)}$ is the supersaturation ratio, with $p_s(T_v)$ the saturation pressure at temperature T_v.

The rate of nucleation is calculated from classical theory, modified to include non-isothermal effects:[13,14]

$$J_* = \frac{q_c}{1+\theta} \frac{\rho_v}{\rho_l} \sqrt{\frac{2\sigma}{\pi m^3}} \exp\left(-\frac{4\pi r_*^2 \sigma}{3kT_v}\right) \quad , \tag{13}$$

where q_c is the condensation coefficient, m the mass of a single molecule and k is the Boltzmann constant. The condensation coefficient is typically equal to 1, even if values between 0.02 and 1.5 have been reported in the literature, as discussed in the Introduction. A review of the different values reported in the literature for the water condensation coefficient is provided in[4] The nonisothermal correction factor θ is equal to:

$$\theta = \frac{2(\gamma - 1)}{1 + \gamma} \frac{h_{vl}}{RT_v} \left(\frac{h_{vl}}{RT_v} - 0.5\right) \quad . \tag{14}$$

Following a modified form of Gyamarthy's formula, the growth rate is given by:[6,15]

$$G = \frac{k_v \Delta T (1 - r_*/r)}{\rho_l \, h_{vl} \, (r + 1.89(1-\nu)\lambda_v / Pr_v)} \quad , \tag{15}$$

with Pr_v the Prandtl number of the vapour, k_v the vapour thermal conductivity and λ_v the mean free path of a vapour molecule, defined as

$$\lambda_v = \frac{1.5 \mu_v \sqrt{RT_v}}{p} \quad , \tag{16}$$

where μ_v is the vapour dynamic viscosity. The parameter ν is a correction given by White and Young[16] for low-pressure nozzles:

$$\nu = \frac{RT_s(p)}{h_{vl}} \left[\beta - 0.5 - \frac{2 - q_c}{2q_c} \frac{\gamma + 1}{2(\gamma - 1)} \frac{RT_s(p)}{h_{vl}}\right] \quad , \tag{17}$$

where β is an empirical parameter, which is typically taken between 0 and 5. Although this correction may be justified on physical grounds (if the condensation and evaporation coefficients were to differ under non-equilibrium conditions), effectively it introduces a modifiable constant, which is often simply adjusted to give agreement with experiments.[13]

Once μ_3 is determined, and therefore y, it is possible to proceed to the computation of the mixture conservation equations and no further moment equations need to be solved.

2.1.3 Closure of Moment Equations

The closure of the moment equations strictly depends on the representation of the droplet growth rate G. If a linear relation is adopted, as:

$$G = a_0 + a_1 r \quad , \tag{18}$$

the integral in equation (10) is replaced by a linear combination of μ_j and μ_{j-1}. Here, the droplet growth is approximated by a constant growth rate:

$$G = a_0 \quad \text{with} \quad a_0 = G(r_{20}) \quad , \tag{19}$$

where r_{20} is the local surface-averaged radius given by:

$$r_{20} = (\mu_2/\mu_0)^{1/2} \quad . \tag{20}$$

This choice is motivated by a superior numerical robustness, even if the accuracy in the transient is reduced. Note that for μ_0, independent of the choice of G the integral of the RHS of equation (10) vanishes since $j = 0$.

2.2 Thermodynamic models

The thermodynamic behavior of the vapor phase is represented by the Z-factor equation of state proposed by Young:[6]

$$Pv = RT(1 + Z) \quad , \tag{21}$$

where the Z is a compressibility parameter designed to account for deviations from perfect gas behavior. In low pressure steam (below 10 bar), an accurate expression for Z is

$$Z = -1.439 \cdot 10^6 \, T^{-5.2} \, P^{1.08} \quad . \tag{22}$$

For the liquid phase, two models are considered: a simple constant-density approximation, and a more realistic temperature-dependent density. Specifically, in the second-case, the following relation is used, taken from Gerber and Kermani:[17]

$$\rho_l = \sum_{i=0}^{3} a_i \, \tau^i \quad , \tag{23}$$

where

$$\tau = \frac{T}{647.286}$$

and

$$a_0 = 928.08\,, \qquad a_1 = 464.63\,, \qquad a_2 = -568.46\,, \qquad a_3 = -255.17 \quad .$$

2.2.1 Quasi-1D Flow

The nozzle flows considered in this paper are described by a quasi-1D model. With this approximation, the velocity field $\mathbf{u}$ reduces to the scalar field u. Due to the area variation, typical of quasi-1D flow, a source term must be introduced on the right-hand side of the Euler equations (1-3):

$$\mathbf{S_A} = \begin{pmatrix} S_{A1} \\ S_{A2} \\ S_{A3} \end{pmatrix} = \begin{pmatrix} -\frac{\rho_m\, u}{A(x)} \frac{\mathrm{d}A}{\mathrm{d}x} \\ -\frac{\rho_m\, u^2}{A(x)} \frac{\mathrm{d}A}{\mathrm{d}x} \\ -\frac{\rho_m\, u\, E + p\, u}{A(x)} \frac{\mathrm{d}A}{\mathrm{d}x} \end{pmatrix} \quad , \tag{24}$$

where $A(x)$ is the area, $\mathrm{d}A/\mathrm{d}x$ its variation. Similarly, a source term must also be introduced on the right-hand side of the transport equations (10):

$$\mathbf{ST_A} = \begin{pmatrix} ST_{A1} \\ ST_{A2} \\ ST_{A3} \\ ST_{A4} \end{pmatrix} = \begin{pmatrix} -\frac{\rho_m\, u\, \mu_o}{A(x)} \frac{\mathrm{d}A}{\mathrm{d}x} \\ -\frac{\rho_m\, u\, \mu_1}{A(x)} \frac{\mathrm{d}A}{\mathrm{d}x} \\ -\frac{\rho_m\, u\, \mu_2}{A(x)} \frac{\mathrm{d}A}{\mathrm{d}x} \\ -\frac{\rho_m\, u\, \mu_3}{A(x)} \frac{\mathrm{d}A}{\mathrm{d}x} \end{pmatrix} \quad . \tag{25}$$

3 NUMERICAL METHOD

In this section the approximation scheme used to discretize the governing equations is presented and details of the treatment for the source terms in the moment transport equations are provided.

3.1 Deterministic wet-steam solver

The governing equations are discretized using a cell-centred finite volume scheme of third-order accuracy, extended to the computation of flows with an arbitrary equation of state.[18] The scheme is constructed by correcting the dispersive error term of second-order-accurate Jameson's scheme.[19] The use of a scalar dissipation term simplifies the scheme implementation with complex equations of state and reduces computational costs. In order to speed up convergence to the steady state and increase robustness, a different approach has been used here for time integration, respect the previous work[1] where an explicit four-stage Runge–Kutta scheme was implemented. The governing equations are integrated in time using an implicit Euler scheme using a defect correction technique. The implicit phase relies on a robust upwind treatment of the convective terms and leads to a

totally discrete scheme which is unconditionnally linearly stable. This allows the use of a CFL number of at least 2 orders of magnitude greater than with the explicit scheme. Local time-stepping is also used to efficiently drive the solution to the steady state.

The main set of the Euler equations for the two-phase mixture (1-3) and the auxiliary set of transport equations (represented by the j^{th} equation (10), with $j = 0, \ldots, 3$) for the droplet distribution spectra are solved by means of an uncoupled procedure: at each time step the properties of the mixture are first computed by solving the main equations with the droplet properties held constant; then the auxiliary equation are solved by using the constant mixture properties. Due to mechanical equilibrium, the pressure field is assumed to be the same for both phases (surface tension is neglected).

3.1.1 Source Terms for the Transport Equations

The source terms in the transport equations contribute a substantial stiffness to the system. This is due to the fact that each moment is much bigger than the moments of lower grades. The large source terms such as nucleation and growth rate also contribute to the stiffness. While the nucleation rate J is always positive, the contribution coming from the growth rate G can be either negative or positive in the transient. The solution to the stiffness issue is found by implicitly treating the source terms. To achieve this a semi-implicit approach is adopted, which means that the growth rate is treated implicitly only when it is negative and stability problems arise. Referring to a generic diffential equation in the variable ϕ:

$$\frac{\mathrm{d}\phi}{\mathrm{d}t} = S(\phi)\,\phi \quad , \tag{26}$$

where $S(\phi)$ represents the non-linear source term, it is discretized as follows:

$$\frac{\Delta\phi}{\Delta t} = S(\phi^n)\,\phi^n + S^-(\phi^n)\,\Delta\phi^n \quad , \tag{27}$$

with $S^-(\phi) = \frac{S(\phi)-|S(\phi)|}{2}$ equal to zero if S is positive and equal to S if S is negative. With this splitting approach, an implicit scheme is applied when the source term is negative, an explicit scheme is applied otherwise.

4 UNCERTAINTY QUANTIFICATION METHOD

Recent research by Loeven et al.,[7,8] has developed an efficient non-intrusive variation on the standard Generalized Polynomial Chaos (GPC) method. Based on the idea of a standard chaos transformation, the Probabilistic Collocation Method (PCM) approach consists of two important modifications to the classic method. The first modification is that a chaos version of Lagrange interpolation is used to approximate the chaos polynomial, even with a minimum of two collocation points. The second modification is to use Gaussian quadrature to compute the Galerkin projection and the integration of the distribution function approximation. In terms of calculation cost, both PC methods show

significant improvements over the MC analysis and Moment Methods, and both PC methods demonstrate exponential convergence with respect to the order of the polynomial. It is noted that for increasing values of the polynomial order, the PCM requires more deterministic calculations than in the GPC case. Nevertheless, the non-intrusive nature of the PCM provides a substantial increase in flexibility. The PCM is therefore particularly suited to the study of complex CFD simulations, without requiring modification to the CFD code framework. The PCM is therefore the stochastic method used in the present study.

In practical terms, the Probabilistic Collocation method consists of calculating the deterministic solution at selected points (nodes) in the input distribution, then multiplying the solutions by a weighting function in order to compute output statistical information. As in the GPC method, each input distribution is associated with a corresponding orthogonal polynomial according to the Askey scheme (summarized in Xiu & Karniadakis[20]). For example, in the case of a normal or Gaussian input distribution, the corresponding quadrature polynomial is the Hermite polynomial. Here the PCM is presented considering the case of a continuous uniform random input distribution with a probability distribution defined as: $U(a,b) = \frac{1}{b-a}$ where $a, b \in \mathbb{R}$ correspond to the left and right limits of the input uniform distribution. The corresponding quadrature polynomial is the Legendre polynomial, and Gauss-Legendre chaos quadrature is employed to compute the Galerkin projection. For the case of a velocity field u subjected to random input variable fluctuations $\xi(\theta)$ (where θ represents the random vector), the solution is decomposed into deterministic: $u_i(\mathbf{x}, t)$, and stochastic: $h_i(\xi(\theta))$ parts:

$$u\left(\mathbf{x}, t, \xi(\theta)\right) = \sum_{i=1}^{P_{PCM}} u_i(\mathbf{x}, t)\, h_i(\xi(\theta)) \quad \text{where} \quad h_i(\xi(\theta)) = \prod_{\substack{k=1 \\ k \neq i}}^{N_p} \frac{\xi(\theta) - \xi(\theta_k)}{\xi(\theta_i) - \xi(\theta_k)} \tag{28}$$

where $u_i(\mathbf{x}, t)$ is the is the deterministic solution at the collocation point θ_i. In the PCM, p is the order of the quadrature polynomial and the number of collocation points is given by $P_{PCM} = p^n$, where n represents the number of random input variables. The term h_i is the Lagrange interpolating polynomial chaos of order $N_p = p - 1$ that passes through the P_{PCM} collocation points, with $h_i\left(\xi(\theta_k)\right) = \delta_{ik}$. The collocation points θ_i are chosen such that they correspond to the Gaussian quadrature points, which are simply the roots of the quadrature polynomial. Additionally, in the case of Gauss-Hermite quadrature, the following transformation is required: $\xi(\theta) = \left(\frac{\theta+1}{2}\right)(b-a) + a$.

In the case of multiple uncertain input parameters, the output statistics must be analytically determined with the multivariable PC expansion (c.f. Equation (9), Xiu & Karniadakis[20]) and the standard definitions of the statistical moments. This procedure is relatively time consuming and complex, especially with several uncertain input variables (i.e. high values of s). A more practical approach to determine the solution statistics is to reconstruct the problem using a simple MC method on the Lagrange interpolation equation, denoted the Reconstructed Monte Carlo method (RMC). Once the determin-

istic solution at each collocation point, $u_i(\mathbf{x}, t)$, has been determined, a MC analysis is used to generate a large number, M, of values for $\xi_s(\theta)$, thereby constructing M possible variations of $h_i(\xi(\theta))$. Since Equation (28) is linear in the terms $u_i(\mathbf{x}, t)$, the RMC can be carried out inexpensively for large values of M. The result is a complete set of output solutions, from which the statistical moments can be easily calculated.

5 NUMERICAL RESULTS

The stochastic solver described in the preceding Section is applied to the computation of condensing steam flows through supersonic nozzles. The computational domain corresponds to the divergent part of the nozzle, with sonic conditions imposed at the throat. Specifically, two nozzle configurations are considered, for which experimental data are available in the literature. The first configuration, referred to as Nozzle 1 (taken from Moore et al.[21]) is characterized by an inlet total pressure $p_0 = 0.25$ bar, inlet total temperature $T_0 = 358$ K; Nozzle 2 (corresponding to Nozzle L of Bakhtar and Zidi[22]), has an inlet total pressure $p_0 = 32$ bar and inlet total temperature $T_0 = 544$ K. Nozzle geometries are given in the Appendices. In both cases, the wet steam flow solver is executed on a computational mesh composed by 400 uniformly spaced cells. For both configurations, several stochastic simulations are performed, assuming random variations of the condensation coefficient q_c in the range $[0.3-1]$ and/or of the empirical coefficient β in the range [0-5]. For both parameters, the uniform density probability function is adopted. The stochastic simulations are carried out by means of a third-order chaos polynomial expansion, which provides a satisfactory convergence of the output statistics.[23] The stochastic code is efficiently parallelized to enable simultaneous calculation of all of the deterministic simulations at the collocation points.

5.1 Nozzle 1

Preliminary computations are performed to investigate the effect of different models for the liquid density. The results, shown in Fig. 1, show that for this low-pressure nozzle the solution is essentially independent of the liquid density model. On the contrary, the results display a significant sensitivity to the empirical parameter β: for higher values of β the pressure distribution is closer to the experimental data, and the mean droplet diameter is about 25% higher. Nevertheless, a complete agreement with the experimental drop size is never achieved. To better understand the role of uncertain parameters on the mean solution output, three stochastic computations are carried out. Since the solutions are essentially independent of the thermodynamic model for the liquid density, only results for the variable density model are shown in this Section.

Initially, the effect of a uniform variation of the condensation coefficient q_c on the numerical solution is investigated. The results are represented in Fig. 2. The pressure and wetness fraction distributions along the nozzle exhibit a reduced sensitivity to modeling uncertainties in the nucleation region, with a peak coefficient of variation ($CV = \sigma/\mu$ %)

of the pressure of approximately 1.8%. Nevertheless, CV values of up to 11% are observed for the wetness fraction. The solution is more sensitive in the nucleation region. Downstream of this region, the variaton of the solution drops to negligible values. Uncertainties on the condensation coefficient affect only slightly the final mean diameter of the droplets (about a 2% variation), whereas the supersaturation ratio and the nucleation rate display large variations. According to Bakhtar et al.,[5] this insensitivity to q_c is a fortuitous effect produced by the introduction of the non-isothermal correction in the nucleation rate model. A second series of simulations is carried out for a uniform variation of the β coefficient between 0 and 5 and $q_c = 1$. The results confirm the preliminary deterministic computations about solution sensitivity to the β coefficient (Fig. 3): the maximum CV for the pressure and wetness fraction is now approximately 2.3% for the pressure and 8.8% for the droplet diameter. Large variations are also observed in the nucleation rate and supersaturation ratio distributions. Conversely, the wetness fraction displays similar trends as in the previous computation. Finally, joint variations of both coefficients are taken into account: the results are shown in figure 4. Surprisingly, the results display lower sensitivities when β and the condensation coefficient are varied simultaneously, when considering the wetness fraction distributions. The joint effect of the two parameters is a global delay of nucleation to lower pressures, and a lower CV value of the mean pressure distribution than in the single parameter variation cases. Combining the uncertainties on q_c and β for the low pressure nozzle produces an effect of negative interference.

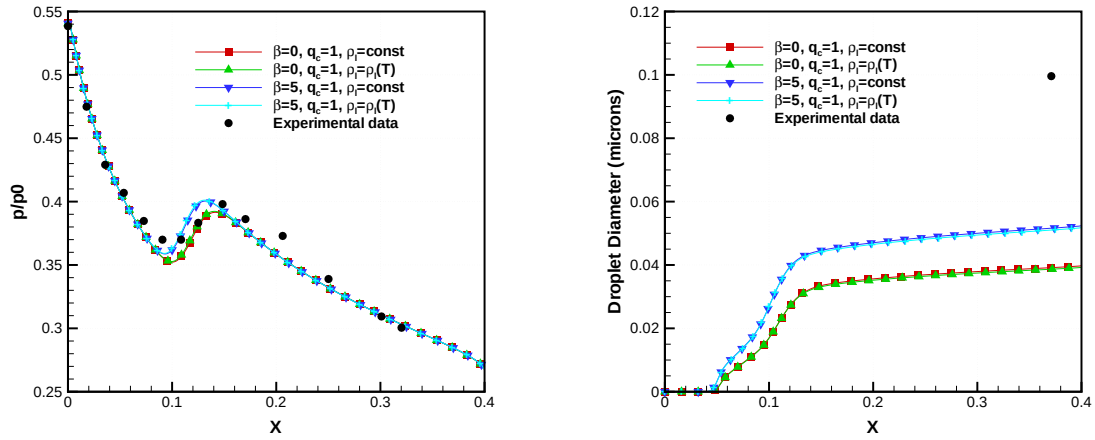

(a) (b)

Figure 1: Nozzle 1, deterministic results for different liquid density models. a) Pressure distribution, b) mean droplet diameter.

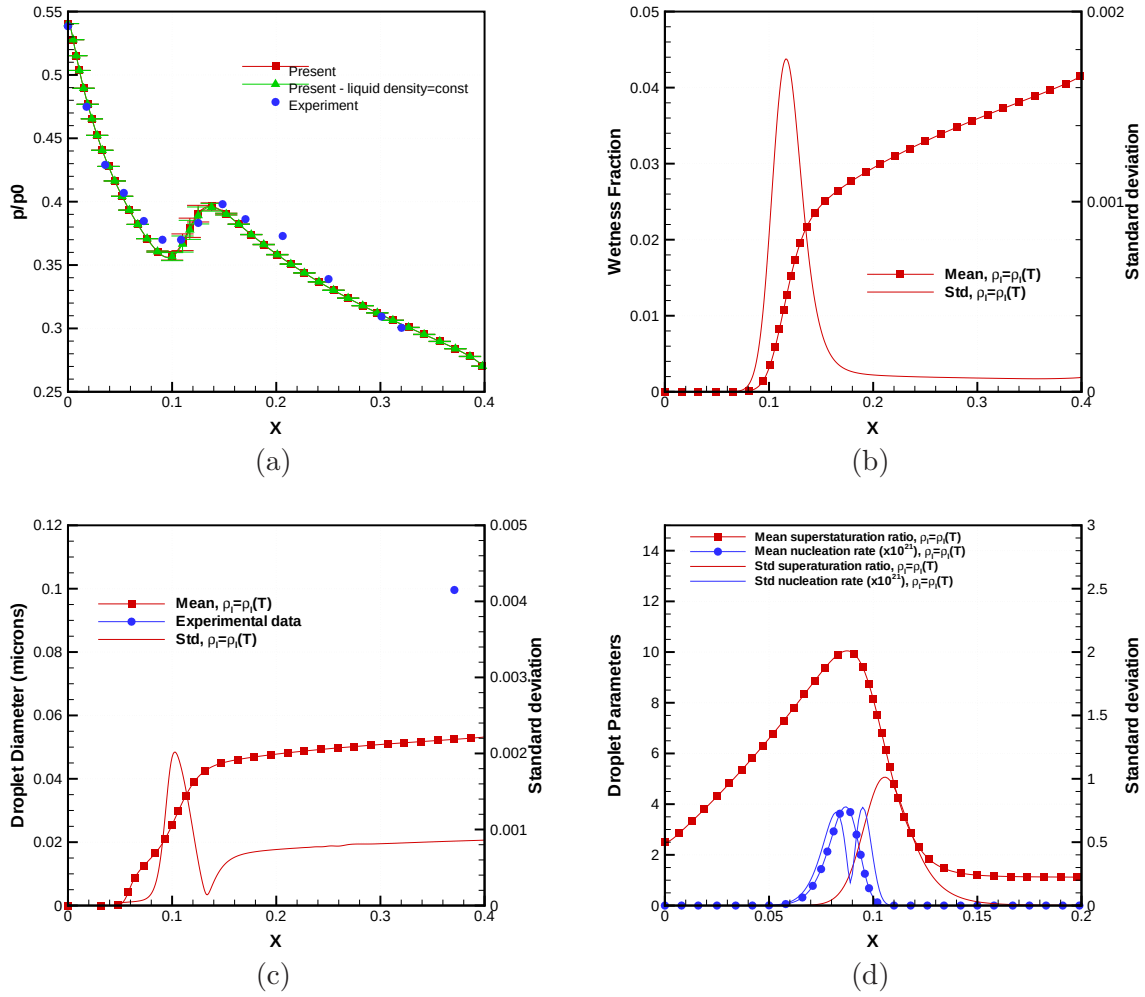

Figure 2: Nozzle 1, stochastic results (mean $\pm\sigma$) for $q_c = U(0.3, 1)$ and $\beta = 5$. a) Pressure distribution, b) wetness fraction, c) mean droplet diameter and d) other wet steam properties.

5.2 Nozzle 2

A high-pressure nozzle is considered with fixed upstream conditions of $p_0 = 32$ bar and $T_0 = 544$ K. Fig. 5 shows preliminary deterministic results obtained for different choices of the liquid density model. Contrary to the preceding configuration, the pressure distribution is now quite sensitive to the density model, which strongly affects the Wilson point location. On the other hand, the results display only low sensitivity to the β parameter. It is important to note that this parameters is simply an *ad hoc* correction for low-pressure models. At higher pressures, the mean free path of the molecules tends toward zero, and the correction term Eqs (15),(17) becomes small. Here again, three stochastic analyses are performed. Initially, β is fixed and a uniform distribution $q_c =$

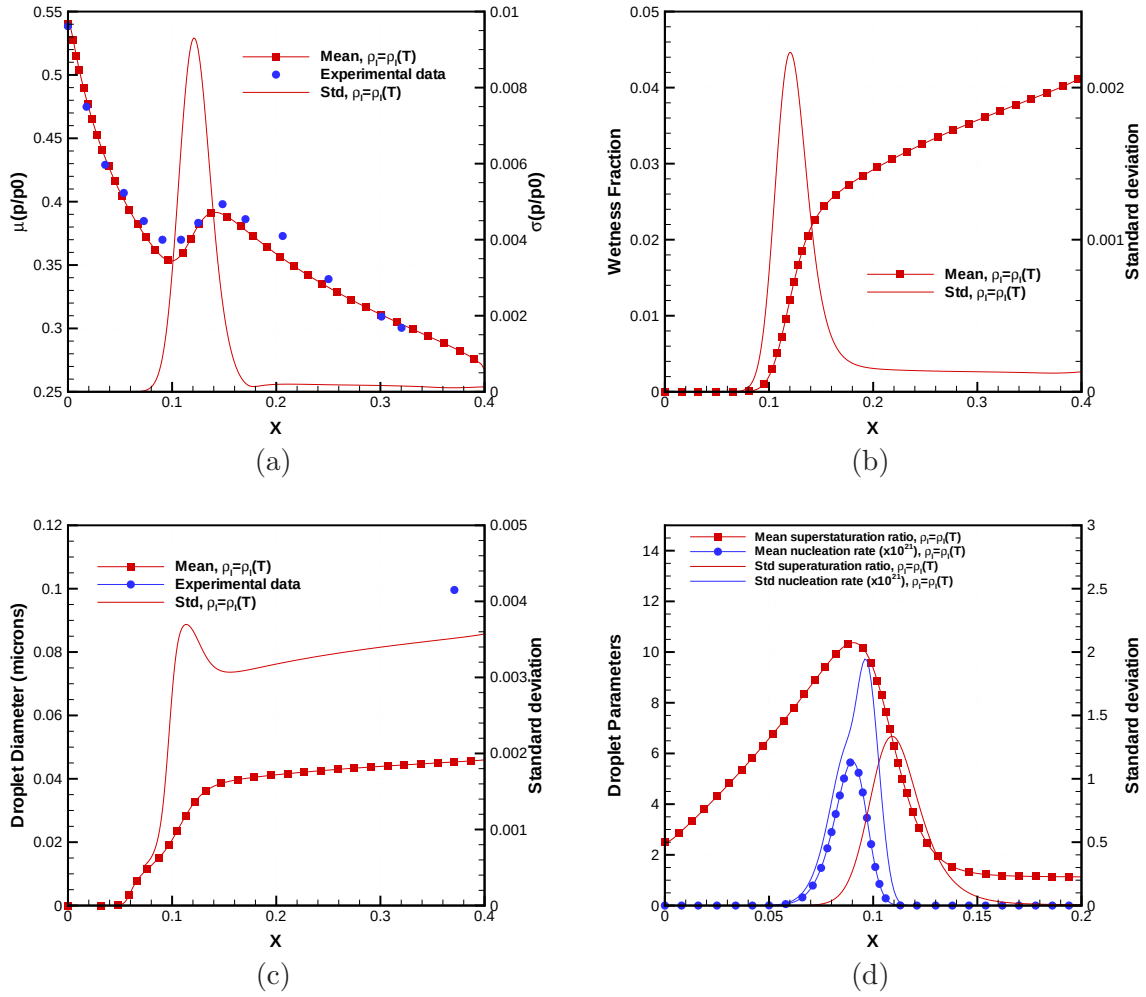

Figure 3: Nozzle 1, stochastic results (mean $\pm\sigma$) for $q_c = 1$ and $\beta = U(0, 5)$. a) Pressure distribution, b) wetness fraction, c) mean droplet diameter and d) other wet steam properties.

$U(0.3, 1)$ is imposed for the condensation coefficient. The numerical results, displayed in Fig. 6, are almost insensitive to q_c. Slightly higher variations are observed when q_c is fixed and equal to one, and the coefficient β is varied with $\beta = U(0, 5)$. In particular, if the pressure and wetness fraction distributions are only slightly affected, the droplet diameter displays variations of more than $CV = 8\%$. Finally, when both coefficients are simultaneously varied ($q_c = U(0.3, 1)$ and $\beta = U(0, 5)$), the system response is amplified, even if the sensitivity of the results to the adjustable coefficients remains quite low. For all of the computed cases, the temperature-dependent density model leads to a somewhat higher sensitivity of the solution to uncertainties in the model constants.

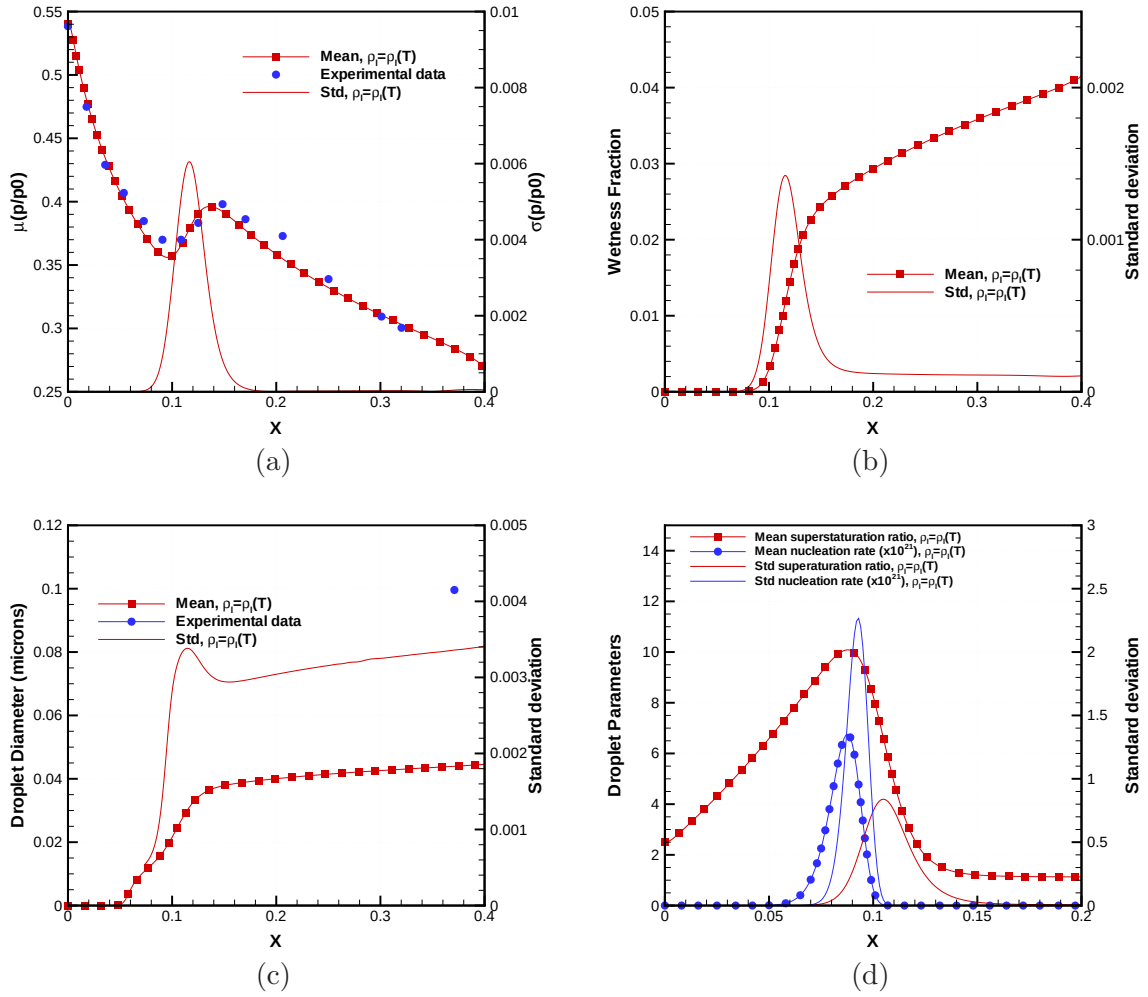

Figure 4: Nozzle 1, stochastic results (mean $\pm\sigma$) for $q_c = U(0.3, 1)$ and $\beta = U(0, 5)$. a) Pressure distribution, b) wetness fraction, c) mean droplet diameter and d) other wet steam properties.

6 CONCLUSIONS

An analysis of the sensitivity of a wet-steam flow solver to uncertainties in the droplet growth and nucleation models was carried out using a stochastic approach. To this purpose, a wet-steam flow solver was coupled to a Probabilistic Collocation Method. For the low-pressure nozzle, the results display a modest sensitivity to the water condensation coefficient q_c, for which very different values have been reported in the literature. On the other hand, the solution displays a quite significant sensitivity to a modifiable empirical constant parameter (noted β) added in the droplet growth model to improve the agreement with experimental results. The results also show that the optimal value of this parameter depends on the condensation coefficient, since simultaneous variation of

both parameters leads to mean solutions in better agreement with experimental data than when only β is adjusted. This suggests that if more accurate estimates of the q_c coefficient were available for low-pressure nozzle, the use of an empirical correction would probably become unnecessary. For high-pressure nozzle, uncertainties on both parameters considered in the present analysis have a marginal effect on the computed solution. In this case, the model is affected much more strongly by the thermodynamic models used to describe the fluid mixture. In particular, the use of a more accurate model for the liquid density improves the agreement of the computed solution with the experimental data, even if the equation of state for the vapor also plays a crucial role (see e.g. Giordano et al.[24]). For both the low-pressure and high-pressure nozzles the results are in quite satisfactory agreement with experiments as far as global mixture properties (such as the pressure) are concerned, the more accurate results being obtained at low pressures. On the contrary, the liquid phase properties, and namely the mean droplet diameter, exhibit large errors compared to experimental data. Nevertheless, the solver captures well the order of magnitude of the generated droplets, which is sufficient to provide valuable information for engineering problems.

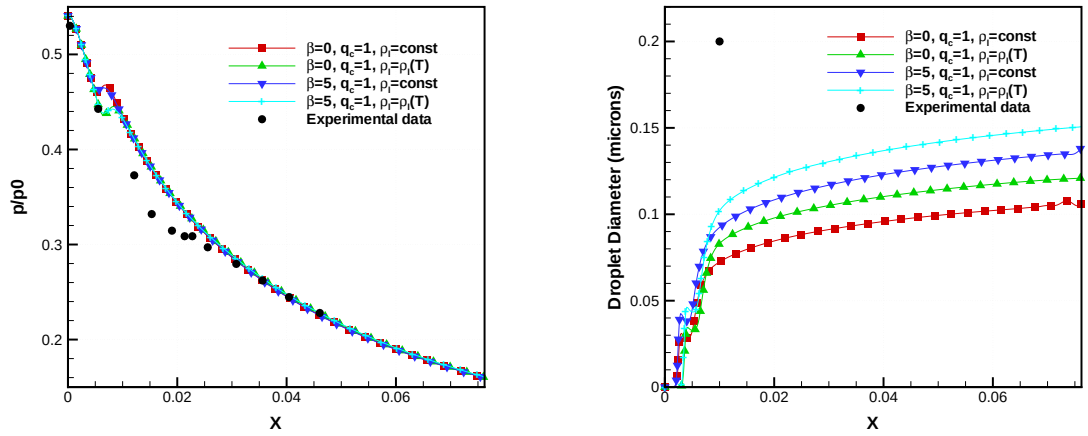

(a) (b)

Figure 5: Nozzle 2, deterministic results for different liquid density models. a) Pressure distribution, b) mean droplet diameter.

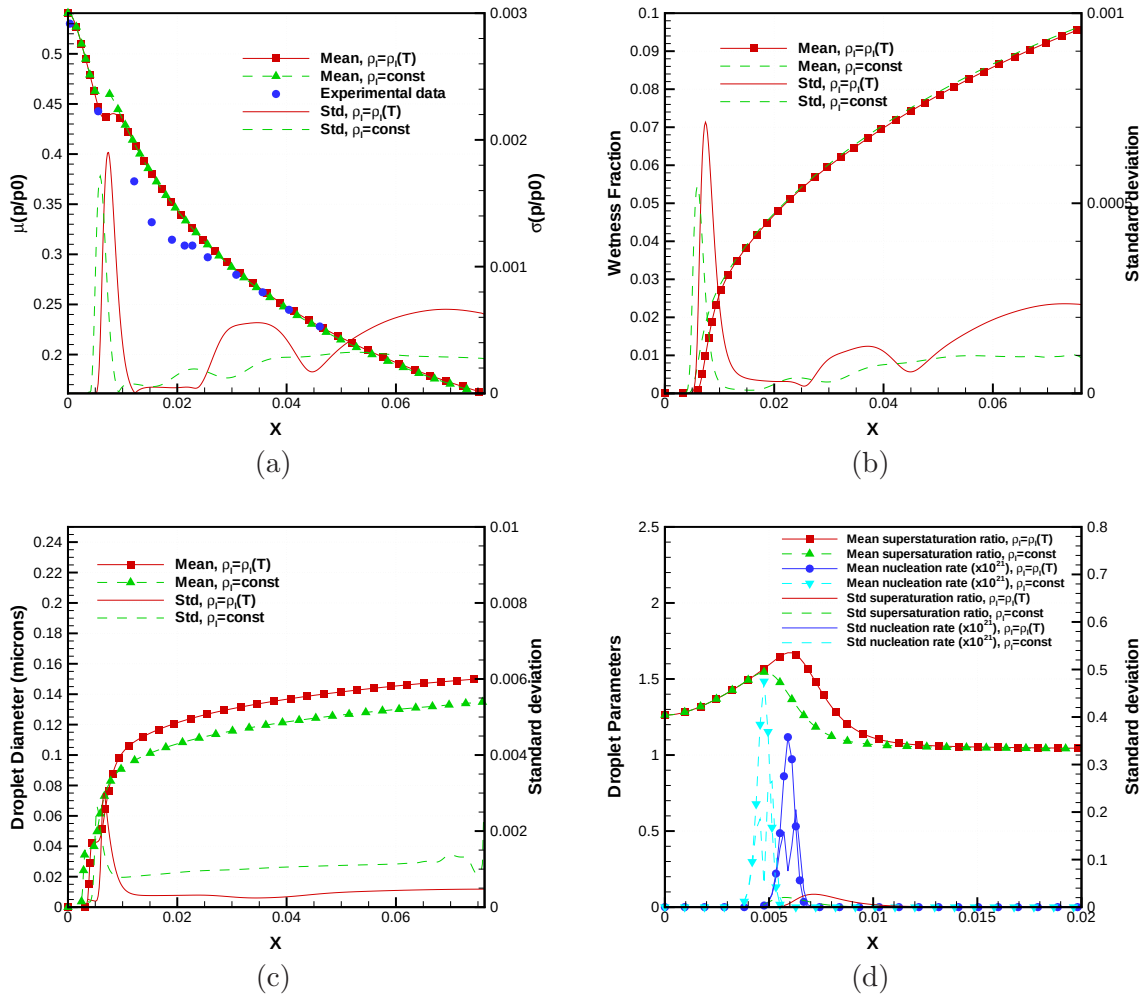

Figure 6: Nozzle 2, stochastic results (mean $\pm\sigma$) for $q_c = U(0.3, 1)$ and $\beta = 5$. a) Pressure distribution, b) wetness fraction, c) mean droplet diameter and d) other wet steam properties.

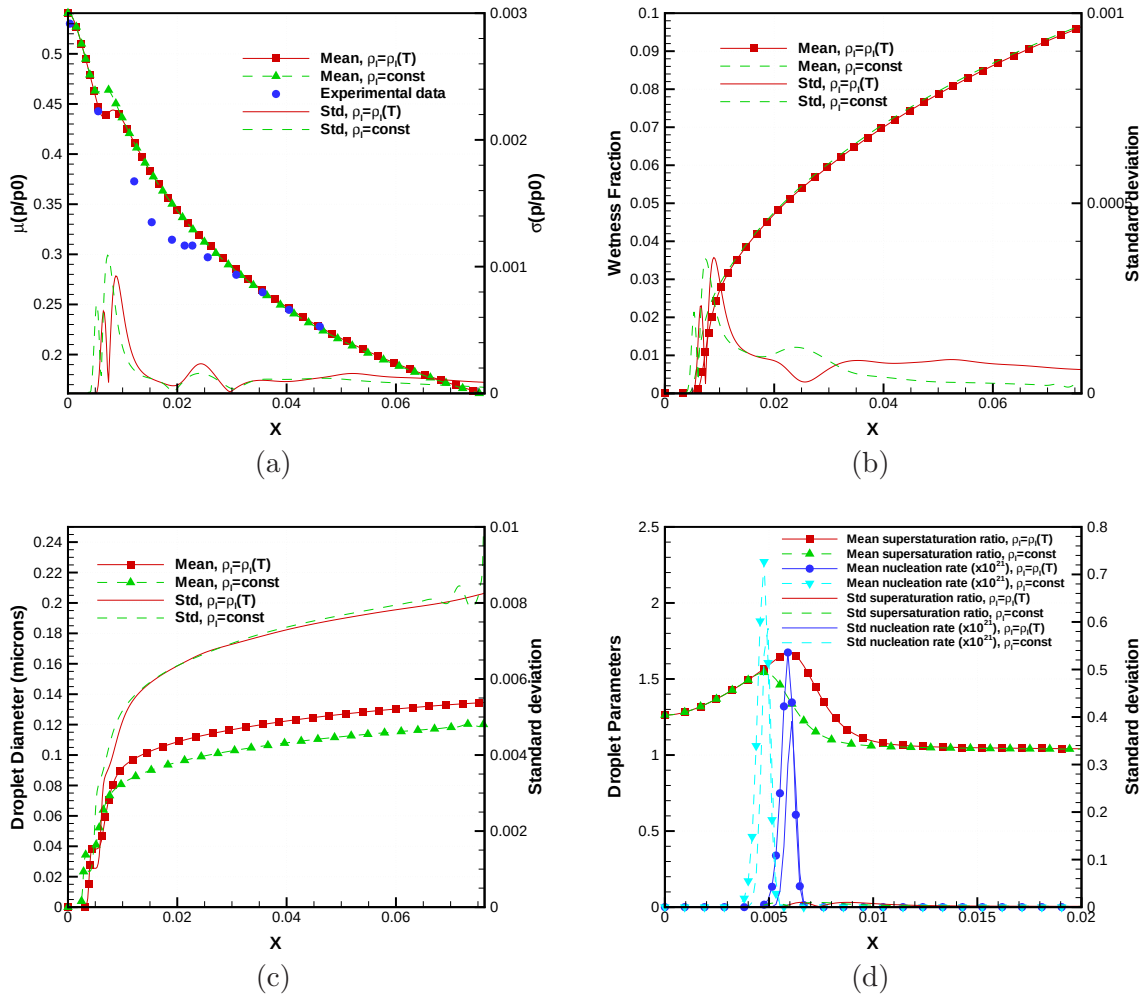

Figure 7: Nozzle 2, stochastic results (mean $\pm\sigma$) for $q_c = 1$ and $\beta = U(0, 5)$. a) Pressure distribution, b) wetness fraction, c) mean droplet diameter and d) other wet steam properties.

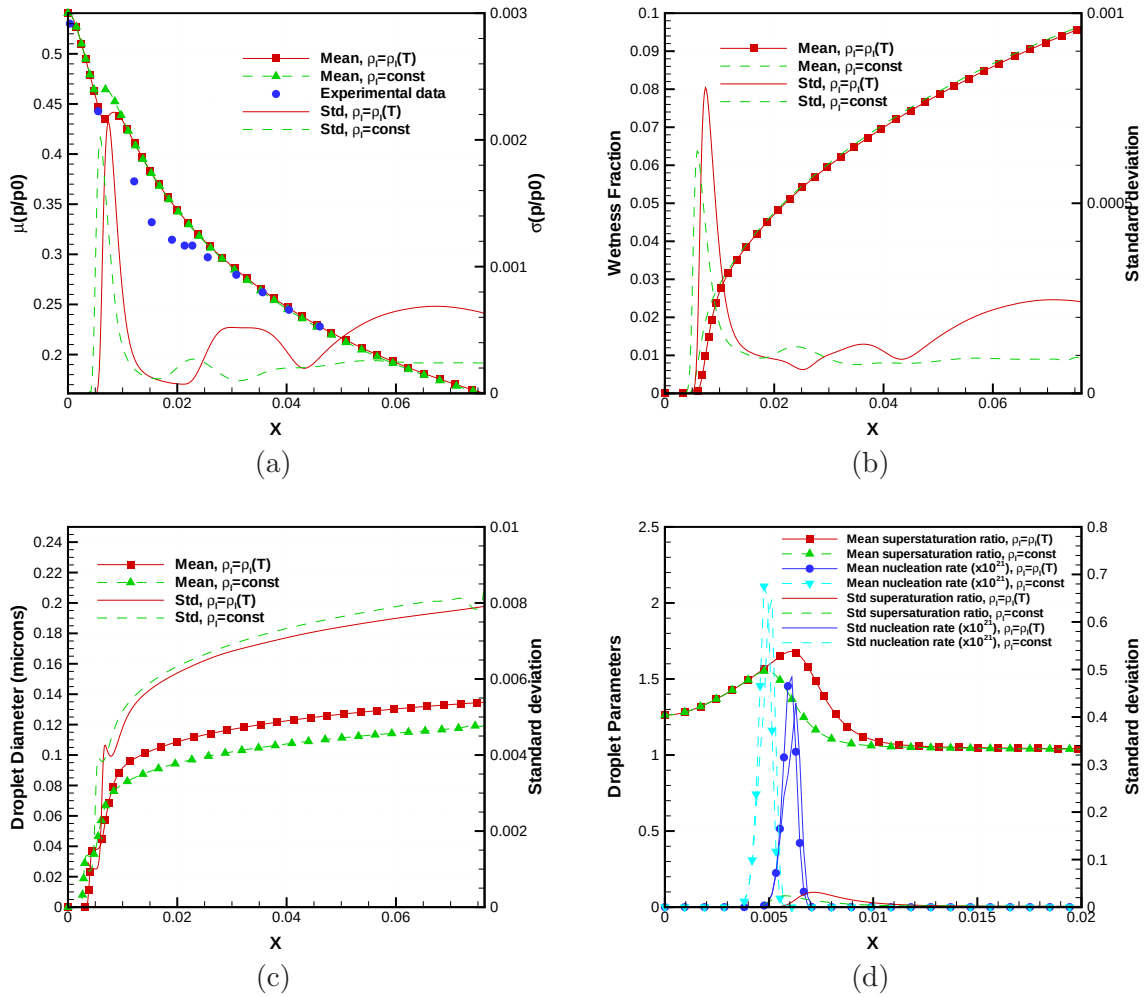

Figure 8: Nozzle 2, stochastic results (mean $\pm\sigma$) for $q_c = U(0.3, 1)$ and $\beta = U(0, 5)$. a) Pressure distribution, b) wetness fraction, c) mean droplet diameter and d) other wet steam properties.

REFERENCES

[1] M. Giordano and P. Cinnella. Numerical method for wet-steam flows with polydispersed droplet spectra. *AIAA Paper 2008-3843* (June 2008).

[2] T. Alty and C. MacKay. Accommodation coefficient and the evaporation coefficient of water. In Proc. R. Soc., vol. A14, 104 (1935).

[3] A. Mills and R. Seban. The condensation coefficient of water. *Int. J. Heat and Mass Transfer*, **10**, 1815–1827 (1967).

[4] M. Mozurkevitch. Aerosol growth and the condensation coefficient of water: a review. *Aerosol Sci. Technol.*, **5**, 223–236 (1986).

[5] F. Bakhtar, J. B. Young2, A. J. White and D. A. Simpson. Classical nucleation theory and its application to condensing steam flow calculations. *J. Mechanical Engineering Science*, **219, Part C**, 1315–1333 (2005).

[6] J. B. Young. Two-dimensional, nonequilibrium wet-steam calculations for nozzles and turbine cascades. *Journal of Turbomachinery*, **114**, 569–578 (1992).

[7] A. Loeven, J. Witteveen and H. Bijl. Efficient uncertainty quantification using a two-step approach with chaos collocation. In ECCOMAS CFD. TU Delft, Netherlands (2006).

[8] A. Loeven, J. Witteveen and H. Bijl. Probabilistic collocation: An efficient non-intrusive approach for arbitrarily distributed parametric uncertainties. In 45th AIAA Aerospace Sciences Meeting and Exhibit, AAIA Paper 2007-317. Reno, Nevada, USA (2007).

[9] P. Cinnella, P. Congedo, L. Parussini and V. Pediroda. Quantification of thermodynamic uncertainties in real-gas flows. *Intern. J. of Engin. Sys. Model. Sim.*, **2**(1-2), 12–24 (2009).

[10] A. J. White. A comparison of modelling methods for polydispersed wet-steam flow. *International Journal for Numerical Methods in Engineering*, **57**, 819–834 (2003).

[11] P. G. Hill. Condensation of water vapour during supersonic expansion in nozzles. *Journal of Fluid Mechanics*, **25(3)**, 593–620 (1966).

[12] A. J. White and M. J. Hounslow. Modelling droplet size in polydispersed steam flows. *International Journal of Heat and Mass Transfer*, **43**, 1873–1884 (2000).

[13] D. A. Simpson and A. J. White. Viscous and unsteady flow calculations of condensing steam in nozzles. *International Journal of Heat and Fluid Flow*, **26**, 71–79 (2005).

[14] A. Kantrowitz. Nucleation in very rapid vapour expansions. *Journal of Chemical Physics*, **19**, 1097–1100 (1951).

[15] A. G. Gerber and A. Mousavi. Application of quadrature method of moments to the polydispersed droplet spectrum in transonic steam flows with primary and secondary nucleation. *Applied Mathematical Modeling*, **31**, 1518–1533 (2007).

[16] A. White and J. Young. Time-marching method for the prediction of two-dimensional, unsteady flows of condensing steam. *J.Propul.Power*, **9**, 579–587 (1993).

[17] A. G. Gerber and M. J. Kermani. A pressure based eulerian-eulerian multi-phase model for non-equilibrium condensation in transonic steam flow. *International Journal of Heat and Mass Transfer*, **47**, 2217–2231 (2004).

[18] P. Cinnella and P. M. Congedo. Numerical solver for dense gas flows. *AIAA Journal*, **43**, 2457–2461 (2005).

[19] A. Jameson, W. Schmidt and E. Turkel. Solutions of the euler equations by finite volume methods using runge-kutta time-stepping schemes. *AIAA Paper 81-1259* (June 1981).

[20] D. Xiu and G. Karniadakis. Modeling uncertainty in flow simulations via generalized polynomial chaos. *J Comput Phys*, **187**, 137–167 (2003).

[21] M. Moore, P. Walters, R. Crane and B. Davidson. Predicting the fog drop size in wet steam turbines. In Wet Steam 4 Conference, 101–109. University of Warwick, Institute of Mechanical Engineers (UK) (1973).

[22] F. Bakhtar and K. Zidi. Nucleation phenomena in flowing high-pressure steam, part, 2: theoretical analysis. In Proc.Instn. Mech. Engrs., vol. 204, 233–242 (1990).
[23] S. Hercus. Uncertainty quantification in the numerical simulation of complex aerodynamic flows. Master's thesis, Arts et Métiers ParisTech, Paris, France (2009).
[24] M. Giordano, P. Congedo and P. Cinnella. Nozzle shape optimization for wet-steam flows. *AIAA Paper 2009-4157* (June 2009).

Appendix A: Nozzle 1 Geometry

The nozzle geometry of the baseline configuration for Nozzle 1 is given by the following third degree polynomial:

$$A(x) = \begin{cases} a_0 + b_0 x + c_0 x^2 + d_0 x^3 & \text{if} \quad 0 \leq x \leq 0.1046 \\ a_1 + b_1 x + c_1 x^2 + d_1 x^3 & \text{if} \quad 0.1046 \leq x \leq 0.2653 \\ a_2 + b_2 x + c_2 x^2 + d_2 x^3 & \text{if} \quad 0.2653 \leq x \leq 1 \end{cases}, \tag{29}$$

where x is expressed in m and $A(x)$ in m^2, and the coefficients are equal to

i	a_i	b_i	c_i	d_i
0	$1.52 \cdot 10^{-2}$	$-2.08 \cdot 10^{-4}$	$1.078 \cdot 10^{-1}$	-0.561
1	$1.533 \cdot 10^{-2}$	$3.21 \cdot 10^{-3}$	$0.419 \cdot 10^{-2}$	$0.47 \cdot 10^{-3}$
2	$1.4926 \cdot 10^{-2}$	$0.59 \cdot 10^{-2}$	$0.871 \cdot 10^{-5}$	$-1.318 \cdot 10^{-5}$

Appendix B: Nozzle 2 Geometry

The nozzle geometry of the baseline configuration for Nozzle 2 is given by the following third degree polynomial:

$$A(x) = \begin{cases} a_0 + b_0 x + c_0 x^2 + d_0 x^3 & \text{if} \quad 0 \leq x \leq 0.041837 \\ a_1 + b_1 x + c_1 x^2 + d_1 x^3 & \text{if} \quad 0.041837 \leq x \leq 0.10612 \\ a_2 + b_2 x + c_2 x^2 + d_2 x^3 & \text{if} \quad 0.10612 \leq x \leq 0.4 \end{cases}, \tag{30}$$

where x is expressed in m and $A(x)$ in m^2, and the coefficients are equal to

i	a_i	b_i	c_i	d_i
0	$1.52 \cdot 10^{-2}$	$-5.1996 \cdot 10^{-4}$	$6.7416 \cdot 10^{-1}$	-8.7727
1	$1.533 \cdot 10^{-2}$	$8.0338 \cdot 10^{-3}$	$2.6189 \cdot 10^{-2}$	$7.3488 \cdot 10^{-3}$
2	$1.4926 \cdot 10^{-2}$	$1.4733 \cdot 10^{-2}$	$5.4451 \cdot 10^{-5}$	$-2.0589 \cdot 10^{-4}$